Development of advanced models for transition to turbulence in hypersonic flows and prediction of transition under uncertainties

Gennaro Serino

Aeronautics and Aerospace Department, gennaro.serino@vki.ac.be

Supervisors: Thierry E. Magin & Patrick Rambaud

Associate Professors, Aeronautics and Aerospace Department, thierry.magin@vki.ac.be, patrick.rambaud@vki.ac.be.

Promoter: Vincent Terrapon

Assistant Professor, Aerospace and Mechanical Engineering Department, University of Liege, vincent.terrapon@ulg.ac.be.

Abstract

A probabilistic approach, based on Uncertainty Quantification, is combined to deterministic numerical simulations relying on Linear Stability Theory and Reynolds Averaged Navier-Stokes. The objective is to improve the prediction of natural transition in hypersonic flows. Results are compared to experimental data obtained in the VKI-H3 facility focusing on the transition onset location and on the extension of the transitional zone. Comparisons show that the computed intermittency distribution is able to capture the experimental onset of transition well following the experimental data within the transitional zone. Finally, a preliminary investigation on the distribution of the perturbation spectrum upstream of the transition onset is also performed with satisfying results.

Keywords: Laminar to turbulent transition, hypersonic flows, Uncertainty Quantification, Linear Stability Theory, Reynolds Averaged Navier-Stokes, intermittency factor, inverse problem, MCMC.

Nomenclature

Symbols

A_0	initial amplitude of the disturbances
M	Mach number
N	amplification ratio
N_{crit}	critical N for transition onset
F	dimensional frequency (kHz)
Re	Reynolds number
St	Stanton number
p_T	probability of transition
$\hat{v}(y)$	amplitude of the perturbations
x	streamwise coordinate (m)
y	normal coordinate (m)
z	spanwise coordinate (m)

Greek symbols

α	streamwise wave number
β	spanwise wave number
δ_{μ_F}	MCMC increment for the mean
δ_{σ_F}	MCMC increment for the variance
γ	intermittency factor
μ	mean
ω	non-dimensional frequency
σ	variance

Abbreviation

CFD	Computational Fluid Dynamics
DNS	Direct Numerical Simulations
$MCMC$	Markov chain Monte Carlo
QoI	Quantity of Interest
$RANS$	Reynolds Averaged Navier-Stokes
TPS	Thermal Protection System
UQ	Uncertainty Quantification
VKI	von Karman Institute for Fluid Dynamics
cdf	cumulative distribution function
pdf	probability distribution function

1. Introduction

During reentry, space vehicles are subjected to an extreme thermal environment due to the deceleration

at the impact with the atmosphere. They are therefore equipped with heat shields which assure the structural integrity. It is well known that heat fluxes in turbulent flows are several times higher than in the laminar regime, thus transition to turbulence plays a key role in hypersonic reentry.
Highly conservative safety margins are currently used in the design of heat shields to take into account unexpected transition due to the variability of the physical environment. The conservative approach allows engineers to take into account variations of the freestream parameters or of the surface geometry but at the expense of a significant increase in their weight. In fact, a change of the Mach number or of the Reynolds number with respect to the design conditions, as well as the presence of roughness or misaligned tiles on the body, can promote transition causing dramatic changes in the predicted heat transfers and faster consumptions of the TPS.
In this research, uncertainties on free stream parameters and surface geometry are taken into account in numerical simulations. The aim is to consider the physical variability of the system to simulate and to study the effect of the uncertainties on some *Quantity of Interest* (QoI). In particular, we focus on the transition location and on the heat loads occurring during atmospheric reentry.
Since transition to turbulence is a stochastic process, deterministic simulations and a probabilistic approach are combined. The latter relies on tools of *Uncertainty Quantification* (UQ) where flight conditions, boundary conditions, or initial disturbances are treated as random and modeled by probability distribution functions (pdf). The objective is to define the probability distribution, and thus confidence levels, on the heat loads and the transition point. Results are then used to improve existing transitional models for a more reliable, faster and less conservative design of the heat shields.

1.1. Motivation of the work

Transition plays a key role in hypersonic reentry affecting the design process of the vehicle. Heat shields guarantee the success of the mission but a conservative design sensibly reduces the space for the payload and increases the weight [6]. An improved understanding of the physics of transition will help to reduce the safety margins and to limit the overall costs of space missions.
Nowadays, we can observe a renewed interest in transition driven by the design of powered hypersonic vehicles as the DARPA FALCON HTV-2 or the ESA IXV. These vehicles are designed to fly at the higher levels of the atmosphere where a laminar or turbulent flow radically affects their drag and required power. Therefore, transition is one of the most important driving factor in the design of reentry vehicles and space planes, from the thermal protection system to the engines.
Experiments and numerical simulations (CFD) are both used to investigate the transition mechanism. In experiments, the freestream parameters, as the Mach and the Reynolds number, can not represent the real flight conditions [1] due to the limitation of the facility and to the physical variability of the environment. In CFD, the real flight conditions can be simulated but models are necessary to represent the physics. These models simplify the more complex mechanisms of transition which makes its prediction less reliable [29].
Transition prediction is therefore characterized by a level of uncertainty which forces engineers to adopt highly conservative safety margins in the design of TPS. A better knowledge of the physics will allow to quantify and eventually reduce these uncertainties leading to a less conservative design to the benefit of safety and costs.

2. Introduction to the deterministic and probabilistic tools

Transition prediction nowadays relies on experiments and numerical simulations. Experimental prediction is done through empirical criteria and correlations (PANT, Shuttle [33]) which have been successfully used in the past. Numerical simulations offer possibilities with different degrees of complexity and costs. Methods for estimating transition in CFD can be based on Linear Stability Theory (LST), Reynolds Averaged Navier-Stokes (RANS) and Direct Numerical Simulations (DNS).
Since linear stability based methods are used for the results hereafter, the fundamentals of the theory will be briefly described. An introduction to the Uncertainty Quantification approach applied to numerical simulations is also given.

2.1. Linear Stability Theory and transition prediction

Most of the current knowledge on hypersonic boundary layer transition is due to the extensive work of Mack [22] and Arnal [2] supported by the

experiments carried out by Stetson [41], Kendall [17] and Schneider [36].

Mack and Arnal focused on modeling the perturbations inside the boundary layer as wave-like disturbances according to the Linear Stability Theory. As described by Schlicthing [35], perturbations are added to the mean flow quantities into the transport equations, which are linearized and combined into the stability equation, called the "Orr-Sommerfeld equation". The solution of this equation gives the parameters, typically the Reynolds numbers and the wave speeds (α), for which the flow becomes unstable. In general, the two-dimensional waves, called the "Tollmien-Schlichting" waves start to grow until their breakdown, which defines the "onset" of transition. This phenomenon is defined as "modal" instability since the perturbations grow exponentially in space and time until transition occurs. When the modal instability does not occur, transition may be caused by the "transient growth" phenomenon where the perturbations grow linearly and then they decay exponentially in time or space. In this case, we speak about "bypass transition" since the modal instability is bypassed in favor of the transient growth which causes transition. The transient growth mechanism is influenced by surface parameters, such as the surface roughness and the wall temperature, and by freestream conditions, such as the turbulence level.

Compressibility effects can be also taken into account in the LST by including additional parameters into the "Orr-Sommerfeld equation". The fundamentals of the LST applied to hypersonic boundary layers were given by the studies and computations of Mack [23], [24]. Mack's greatest contribution was the discovery of multiple solutions of the stability equation in the high-speed regime which were called higher modes or *Mack modes* in his honor. A *first mode* instability is physically related to the generalized inflection point in the boundary layer profiles. It has been shown that when this point exists, the profiles are intrinsically unstable. An intuitive example is the breakdown of the sea waves when they are approaching the land. When the Mach number is higher, a second type, *second mode*, of instability is physically due to the pressure disturbances which are trapped in the boundary layer between the wall and the sonic line. The acoustic waves are continuously reflected, bouncing between the surface and the sonic line until their amplification is high enough to cause transition. This second mode instability is also called "acoustic" or "radiative" instability. In high speed boundary layer, transition is generally due to the second mode instability.

Mack also carried out several studies on the effect of wall cooling on boundary layer stability. In contrast to the early stability theory [20] which considered wall cooling as a complete stabilizer of the boundary layer, Mack found that the higher modes were destabilized in presence of cold surfaces. Thus, a cold surface is characterized by a lower transitional Reynolds number than a hot surface.

Several experiments were carried out to investigate boundary layer instability in high-speed boundary layers. The existence of second mode instabilities was proved by the experiments of Kendall [17] where higher modes were found to be the dominant destabilizing source. Further investigations were carried out by the extensive work of Schneider [36] who focused on hypersonic transition on conical geometries in several wind tunnels. A detailed review, of flight data and experiments carried out in the framework of hypersonic transition can be found in [37].

Experiments are linked to LST through the e^N transition prediction method. It consists in linking the experimental transition onset to the growth of the perturbations through the N-factor [44]. This is an index measuring how much the initial perturbations are amplified along the stream-wise direction. Generally, the N-factor is around $8 \div 9$ at transition onset for low-speed flows while it is around $4 \div 5$ in hypersonic regime due to higher velocities. It also depends on the facility where the test is carried out since it is related to free stream level of noise. In fact, the higher the noise is the lower is the threshold N-factor where transition occurs. As a consequence, transition is usually observed for N-factor around $12 \div 14$ in flight conditions, since the freestream turbulence is really low. For example, Fig. 1 shows the computed N-factor on the HIFire I reentry vehicle in flight conditions given by [11] for different frequencies of the perturbations. The onset of transition was observed at $x = 0.76$ m on the surface model corresponding to a N-factor equal to 13.5. Once the N-factor is known for certain conditions and facilities, transition prediction can be done by computing the growth rate of the perturbations by LST. Thus transition occurs where the computed N-factor is equal to the threshold value. This is known as the e^N transition prediction method, whose practical application is widespread due to its simplicity and reliability. However, its simplicity is also a limitation since it does not take into account effects such as the presence of surface roughness. Moreover, the extension to three-dimensional flows is not straightforward (i.e.

cross flow instabilities). In addition, it requires to know the N-factor at the transition point in advance through calibration and wind tunnel tests. Hence the e^N approach is considered a semi-empirical method.

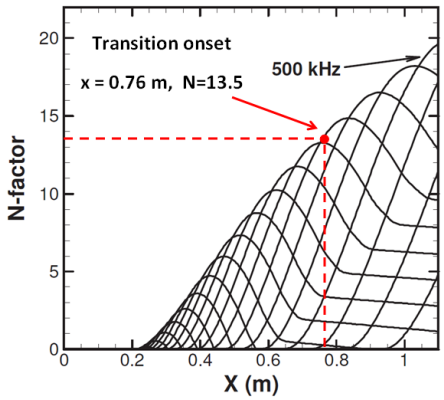

Figure 1: N factors computed on the HIFire I reentry vehicle[11] : $M_\infty = 5.28$, $H = 21$km

2.2. *Uncertainty Quantification and numerical simulations*

Iaccarino *et al.* [18] define Uncertainty Quantification (UQ) as a probabilistic approach to determine confidence levels on the results of numerical simulations. A real physical system is characterized by intrinsic uncertainties related to the input conditions. UQ aims at studying how these uncertainties affect the numerical results focusing on some *Quantities of Interest* (QoI). The typical process consists in characterizing the input uncertainties, then propagating them through the numerical simulation and, finally, defining the margins and error bars on the QoI. For example, in the context of this work, uncertainties on the freestream perturbations or freestream parameters, such as the Mach number and the Reynolds number, are investigated to quantify their effects on the transition onset and length.

UQ has been applied recently to estimate the effects of different parameters on numerical simulations. For instance Pecnik *et al.* [31] study the effects of input uncertainties on transition prediction of transonic gas turbine compressors where numerical results are compared with experimental data obtained at the von Karman Institute for Fluid Dynamics (VKI) for several turbine guide vane test cases. A similar approach has been used by Sankaran [34] for simulations of blood flow in both healthy and diseased vascular models where the effect of hemodynamic parameters including velocities, time varying wall shear stress, pressure drops, and energy losses is investigated. Here, the input uncertainties are quantified and mapped to the stochastic space using the stochastic collocation technique. The idea of stochastic collocation methods is that the points which the model is evaluated at are chosen so that they are orthogonal with the probability distributions on the inputs as a weighting function. A detailed explanation of the method is given by Loeven [21] who also presents a modified version to obtain faster convergence on the results.

The parameters to investigate can be also part of the model used for the numerical simulations. An example can be the values of a parameter of a transition or turbulence model such as the free stream turbulence level or the eddy viscosity ratio. Studies on these type of uncertainties is performed by Gorle [14] in RANS simulations of turbulent mixing. In this study, uncertainties are identified in the Reynolds stresses and in the scalar fluxes. To correctly quantify these uncertainties, perturbations are introduced in the values obtained from the deterministic models with a range of variations based on a comparison with LES data.

Applications of the UQ strategy to high-speed flows are presented by Iaccarino [19] for two classical problems in unsteady compressible fluid dynamics: the Riemann problem and the Woodward-Colella forward step flow. These applications show the advantage of using the probabilistic approach in problems with discontinuities such as shock waves. In Fig. 2, for the Woodward and Colella forward facing step problem, the mean and the variance of the divergence velocity field are represented. It can be noticed how the position of the shock wave and its reflection radically change when uncertainties on the freestream Mach number are considered.

Figure 2: Woodward and Colella forward facing step problem. Mean velocity divergence field corresponding to an uncertain input Mach number [2.5 : 3.0]. Stochastic collocation based on $M = 3$ [19].

The propagation of uncertainties through the computational model can be achieved by either intrusive or non-intrusive techniques. A non-intrusive

technique consists in several repetitions of the original deterministic models. Examples are the Monte Carlo method or the stochastic collocation approaches where the computational model is treated as a black-box and several simulations are performed. On the other hand, an intrusive technique is based on the modification of the original deterministic model, as in the polynomial chaos approach, where a polynomial expansion simplifies the original model. Intrusive techniques suffer strongly from the *curse of dimensionality* since they are slower to converge when the number of parameters increase. In this work, a non-intrusive approach based on stochastic collocation is used.

3. Formulation of the method

This section explains how the deterministic (Sec. 2.1) and the probabilistic tools (Sec. 2.2) are used and combined in the present research.

3.1. Assumptions for the deterministic simulations

LST[35] assumes wave-like disturbances in the mean flow which can be modeled as a function of spatial coordinates x, y, z and of time t :

$$\begin{aligned} v(x,y,z,t) &= \hat{v}(y)e^{i(k\alpha x + l\beta z - m\omega t)}, \\ \alpha = 2\pi/\lambda_x \quad \beta &= 2\pi/\lambda_z \end{aligned} \tag{1}$$

In Eq. 1, x is the streamwise direction, z the spanwise direction and y the direction normal to the wall while α and β are the streamwise and spanwise wave numbers, respectively. $\hat{v}(y)$ is the complex disturbance amplitude while k, l, m are integers representing the different wave numbers along the streamwise, spanwise direction and in time, respectively. The frequency ω is related to the streamwise wave number α by the phase speed c, $c = \omega/\alpha$, at which the disturbances travel downstream. In general, α, β and ω are complex. We consider here that transition is due to *second mode* instabilities so that perturbations are amplified along the stream wise direction x. In this case, β vanishes since the direction of maximum amplification is aligned with the streamwise coordinate x. As the spatial approach is used here, ω is real while α is complex.
Transition is predicted with the $e^N - method$ which is described by Arnal [2] (see Sec. 2.1). In the spatial approach is used, the N factor is obtained by integrating the amplification rates α_i along the streamwise direction :

$$N = log\frac{A}{A_o} = \int_{x_0}^{x} -\alpha_i dx \tag{2}$$

In Eq. 2, A_0 is the initial amplitude of the disturbances at the location x_0 where they start to be amplified. According to the e^N method, transition occurs when the computed N factor equals the value determined at the experimental transition location for a specific wind tunnel. As explained by Arnal [2], the N-factor depends on the facility where the test is carried out. In general, for subsonic facilities, the N factor for transition is around $8 \div 9$ while it is $4 \div 5$ at higher Mach number as in hypersonic regime. Examples of application of the method are the experiments carried out by Horvath [16] in the NASA Langley Mach 6 wind tunnel where transition onset occurs when $N = 3.8$.

3.2. Description of the method

1. Linear stability analysis: freestream conditions and geometrical parameters are defined for a test case and then boundary layer profiles are obtained from self-similar solution or CFD simulations. Then, the stability analysis is carried out by choosing a frequency for the perturbation waves in a given range of variation. For high-speed flows typical frequencies are within $400 \div 800$ kHz. The linear amplification phase is solved with the stability code VESTA developed by Pinna [32] at the VKI. It has been shown by Marxen [27] that LST is a good model for describing the linear amplification of the perturbation waves through comparison with DNS data. At the end of the stability analysis, the N-factor is computed according to Eq. 2. Therefore, the output of this first step is a series of curves describing how the perturbations with different frequencies are amplified along the streamwise direction. This output constitutes the *transfer function* which will be used in the probabilistic approach. An example is shown in Fig. 3 for one of the experimental cases carried out by Masutti [26] in the VKI-H3 facility.
2. Definition of the uncertainties: LST has been carried out by considering the variation of the dimensional frequency (F) of the free stream perturbations. The UQ approach aims at defining how the variation of this parameter affects the

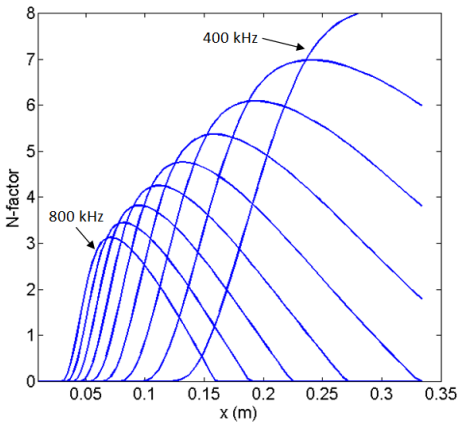

Figure 3: N factors computed on the VKI-H3 High Reynolds case [26]: $M_\infty = 6$, Frequency $\in [400 : 50 : 800]$ kHz.

transition onset location. In order to do that, a probability function (pdf) with a normal distribution is assumed to describe this source of uncertainty. Generally, a normal distribution includes all the possible values of a parameters from $-\infty$ to $+\infty$. In the current work, in order to prevent non physical values, such as negative frequencies, the probability distribution has been truncated into a fixed range. Frequencies are then selected in this range that includes the typical values for *second mode* instability. An example of the pdf for the input uncertainties is shown in Fig. 4.

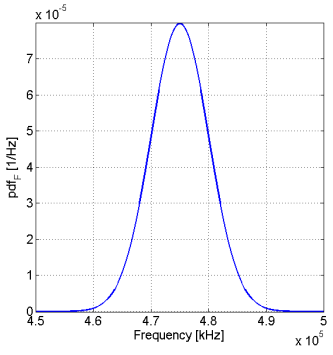

Figure 4: Example of pdf of the input parameter for the UQ analysis

3. Propagation: LST analysis defines a *transfer function* which links the input uncertainty (i.e. the frequency F) to the output (i.e. the N-factor) for the estimation of the transition onset in the simulations. Once the input pdf is assumed, the output pdf is obtained by applying the *method of transformation*. This method is valid as long as the $input - output$ relation is unique, that is when the *transfer function* is monotonic. An illustration of the method is represented in Fig. 5 for generic input, $f(x)$, and transfer function $y(x)$. In our case, the *transfer function* $N = N(F)$ is unique up to the maximum N-factor for each curve which describes the relation between the input frequency F and the output N-factor. The method consists in obtaining the output pdf by multiplying the input pdf and the *Jacobian*, $J(F, N) = dF/dN$, of the *transfer function* as reported in Eq. 3.

$$pdf(N) = J(F, N) \times pdf(F) \tag{3}$$

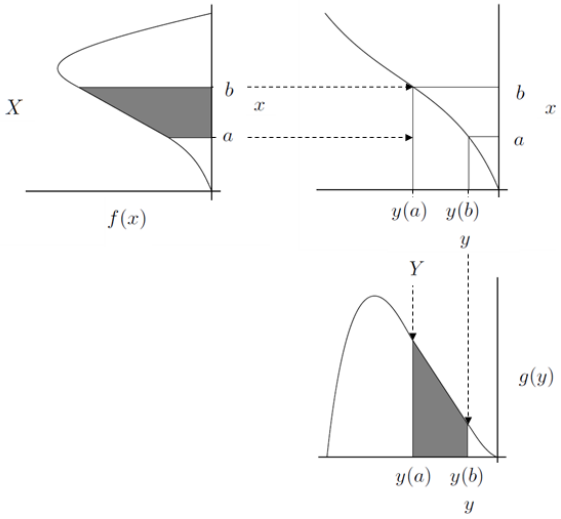

Figure 5: Example of the *method of transformation*

4. Output: the probability distribution of the $N-$factor for each station of the computational domain is the output of the analysis. Since the work aims at modeling the transition region, results are presented in terms of the probability of having transition at a fixed location. This probability is computed by integrating, at a fixed streamwise coordinate, along N up to N_{crit}, which is the N value corresponding to the transition onset experimentally observed. The integration is reported in Eq. 4.

$$p_T = 1 - \int_0^{N_{crit}} pdf(\bar{N}) d\bar{N} = \gamma. \tag{4}$$

The probability of transition starts from 0 where the flow is most likely to be laminar. Then it

gradually rises to 1 where the flow is most likely to be fully turbulent. This probability can be interpreted as the *intermittency factor* γ, which has been defined by Narasihma [30] as the time ratio between turbulent and laminar flow at a fixed location. A summary of the procedure described above is reported in Fig. 6(a), while in fig. 6(b) an example of the output probability of transition is shown.

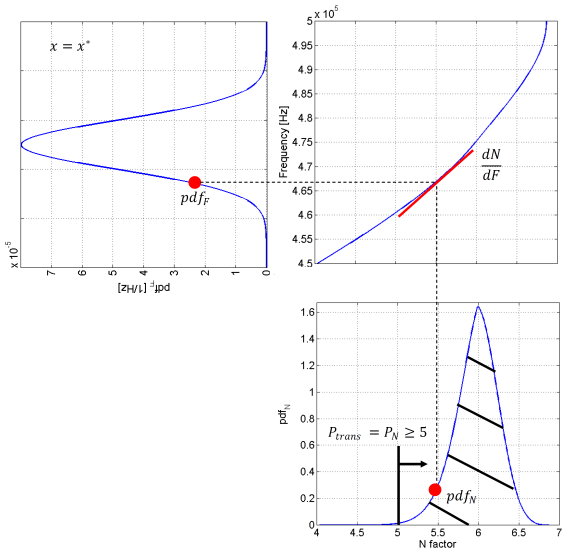

(a)

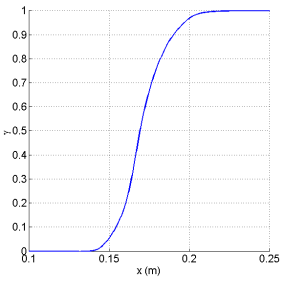

(b)

Figure 6: (a) Summary of the procedure to obtain the probability of transition, (b) Example of probability of transition.

4. The VKI-H3 test case

The assumptions described in Sec. 3.1 have been applied to different test cases with the approach described in Sec. 3.2. Here, a test case for natural transition on a 7° half cone model in the VKI-H3 facility is presented. The test conditions are summarized in Tab. 1 for different Reynolds numbers. Experiments were carried out by Masutti [26] and results are represented in Fig. 7. Transition is detected by surface measurements of the heat flux which is then expressed as the non dimensional Stanton number (St). This number quantifies the amount of heat transfered to the wall of the model. From experimental data, it can be seen that the transition onset location moves upstream as the Reynolds number increases.

The analysis is divided in two parts. The first is focused on studying how the uncertainties on the freestream perturbations propagate to the numerical results and on the comparison between the numerical results and the experimental data. In the second part, an inverse analysis is carried out to investigate the distribution of the freestream perturbations which is most likely to cause transition for one of the cases. The first analysis is also defined as *the forward problem* and it follows the steps described in Sec. 3.2. The second part is called the *the inverse problem* and it will be described in the following sections.

Test case	M_∞	T_∞ [K]	Re_∞ [1/m]	T_w [K]
Low Reynolds	6.0	60	18.0×10^6	294
Medium Reynolds	6.0	60	22.8×10^6	294
High Reynolds	6.0	60	27.1×10^6	294

Table 1: Test case and freestream conditions

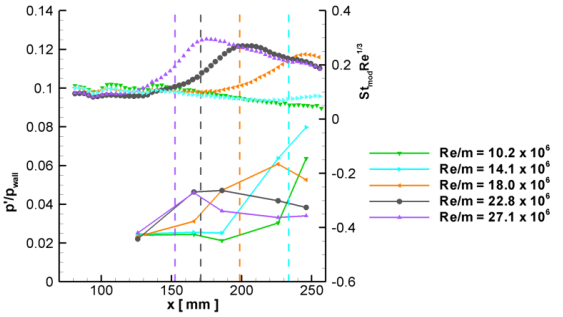

Figure 7: Experimental results obtained in VKI-H3 facility (conditions are given in Tab. 1). Modified Stanton number (top curves) and pressure variations (bottom curves) against the streamwise coordinates

.

4.1. The forward problem

We assume that laminar-turbulent transition is caused by perturbations in the boundary layer upstream of the transition location. The aim of *the forward problem* is to obtain the probability of transition

caused by an assumed free stream perturbation spectrum.

For the conditions indicated in Tab. 1, a linear stability analysis has been carried out and the N-factor has been obtained. Then, a pdf has been assumed for the frequencies which characterize the freestream perturbations. We assume that the pdf is normally distributed around its mean μ_F with a variance σ_F in a given range of frequencies. The value of the mean and the variance are indicated in Tab. 2 for the different Reynolds numbers. The values have been obtained by choosing the mean of frequency distribution such that the amplification ratio reaches the threshold value at the experimental transition onset. It has been found that, in the VKI-H3 facility, the limiting N-factor is equal to 5. In Fig. 8 the isolines of the N-factor are computed for the High Reynolds conditions in which transition is observed at ≈ 0.13 m (see Fig. 7). A mean frequency of 480 kHz with a variance of 25 kHz allows to have a satisfying agreement with the experimental data.

Test case	μ_f [kHz]	σ_F [kHz]	Range [kHz]
Low Reynolds	330	10	200 ÷ 800
Medium Reynolds	410	20	200 ÷ 800
High Reynolds	480	25	200 ÷ 800

Table 2: Parameters for the input pdf

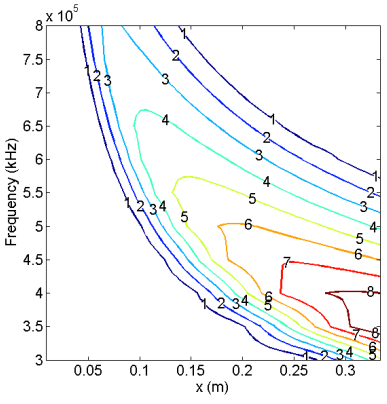

Figure 8: N-factor isolines against Frequency and streamwise coordinate for the High Reynolds condition computed with LST

Experimental data are available in term of Stanton number $St(x)$ (Fig. 7) along the cone model. In order to compare them with our results, the St has been normalized to obtain the experimental intermittency factor γ within the transition region. Since the transition onset x_{onset} and the transition offset x_{offset} are known, the experimental intermittency can be obtained through Eq. 5.

$$\gamma(x) = \frac{St(x) - St_{x=x_{onset}}}{St_{x=x_{offset}} - St_{x=x_{onset}}} \tag{5}$$

The normal distribution with the parameters given in Tab. 2 allows to compute the probability of transition and, thus, the intermittency curves for the different test conditions. Results are represented in Fig. 9 and compared to the experimental data. The transition onset location and the shape of the intermittency factor within the transition region agree very well with the experimental data. For all cases, a characteristic shape is obtained similar to the classical error function. The good agreement with the experimental data demonstrates the validity of the approach and, in particular, confirms the validity of the e^N transition prediction for high-speed flows.

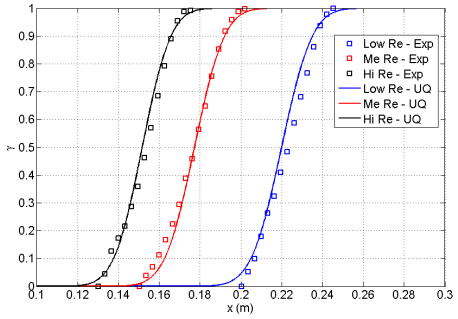

Figure 9: Intermittency as a function of the streamwise location : comparison between UQ analysis (-) and experimental results (□) for the conditions given in Tab. 1.

4.2. The inverse problem

The forward problem described above can be regarded as a computational model $f(s)$ that takes D input parameters $s = (s_1, ..., s_D)$ and produces a K-vector of derived outputs $m = (g_1(f(s), r), ..., g_K(f(s), r))$ with auxiliary parameters $r = (r_1, ..., r_N)$. Solving for m given s is called *the forward problem*, while inferring s given the measurements of m is denoted as *the inverse problem*.

For the test case, the two input parameters are the mean and the variance of the perturbation spectrum of the frequency, so $s_1 = \mu_F$ and $s_2 = \sigma_F$. The auxiliary parameters r correspond to the conditions indicated in Tab. 1. We consider as outputs the probability of transition γ at selected locations $x_1, ..., x_K$ and hence $m = (\gamma_1, ..., \gamma_K)$.

Due to measurement uncertainties, the input quantity s can only be characterized by its statistics, namely the probability $p(s)$. In other words, the mean and variance of the perturbation distribution are themselves probabilistic. The solution of the forward problem hence yields a probability $p(m)$. In the inverse problem, the measurements of m are noisy and the input to the statistical inverse problem is $m+\eta$, where η quantifies this noise. In the inverse problem, we start with a given set of noisy measurements $m+\eta$ and seek the input parameters s using our computational model $f(s)$. The inverse problem is solved by applying the Bayesian inversion. Instead of calculating s, we compute a probability of s given m, $p(s|m)$, which is the so-called *posterior density*. Bayes theorem states that the conditional probability of the parameters s given the measurements m is equal to the product of the probability of the measurements m given the parameters s, times the ratio between the probabilities of the parameters s and the measurements m:

$$p(s|m) = \frac{p(m|s) \times p(s)}{p(m)} \propto p(m|s) \times p(s) \qquad (6)$$

In Eq. 6, $p(s)$ is the *prior probability density* which is related to the information on the input parameters and $p(m|s)$ is the *likelihood probability* which relates the measurements to the input parameters. Finally, $p(m)$ is a normalizing constant that ensures that the product of the likelihood and the prior is a probability density function, which integrates to one.

Several methods are available to infer the posterior probability density. Two such methods are the Markov Chain Monte Carlo (MCMC) method or the Kalman filtering method [42]. The former includes algorithms for sampling from probability distributions based on building a Markov chain that has the desired distribution as its equilibrium distribution. The state of the chain after a large number of steps is then used as a sample of the desired distribution. The quality of the sample improves as a function of the number of steps. For the current application, this method has been implemented and used to compute the posterior probability density $p(s|m)$ with a Metropolis-Hastings algorithm [15]. For simplicity, we assume a Gaussian distribution for the prior probability density $p(s)$. The effect of this assumption will be assessed in future works.

In our specific context, the inverse problem consists in obtaining the distribution of the frequency which gives the intermittency closest to the experimental data. The parameter to be inferred are the mean μ_F and the variance σ_F of the frequency pdf at the transition onset.

This approach has been applied to the VKI-H3 experimental data for the low-Reynolds number case ($Re = 18 \times 10^6$). The inverse problem has been solved by using the Markov-Chain Monte Carlo method where the forward problem is solved several times by varying the input parameters in a given range. Starting from an initial distribution defined by μ_0 and σ_0, successive realizations are obtained with different combinations of the parameters and selected increments (δ_{μ_F}, δ_{σ_F}) for the mean and the variance, respectively. The method guarantees the convergence to the exact solution after a certain number of steps. An illustration of the sampling space is shown in Fig.10 with the starting point (μ_{F0}, σ_{F0}) and the burn in period. The converged mean and variance are evaluated on the remaining samples as represented in Fig.11 and Fig.12. The final values are reported in Tab.3 and compared to the probability distribution previously assumed for the forward problem.

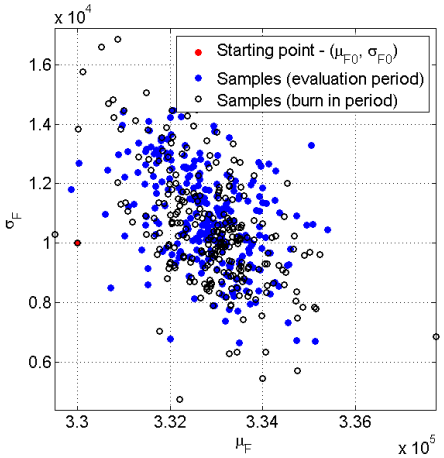

Figure 10: Sampling space : starting point (red), burn in period (black) and useful samples (blue)

Low Reynolds	μ_f [kHz]	σ_F [kHz]	Range [kHz]
Forward problem	330	10	200 ÷ 800
Inverse problem	333	11	200 ÷ 800

Table 3: Comparison of the probability density functions for the forward and the inverse problem in the low Reynolds number case

The posterior probability density is represented in

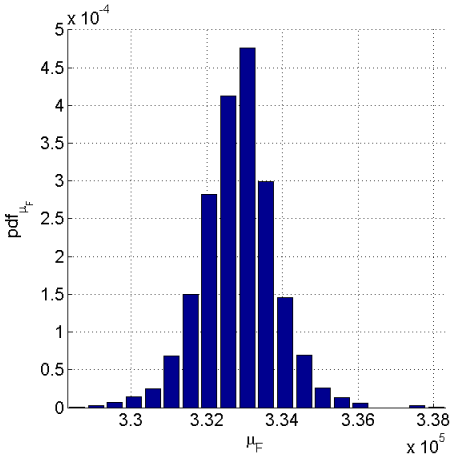

Figure 11: Probability density function for the mean of the frequency (μ_F) for the low Reynolds case

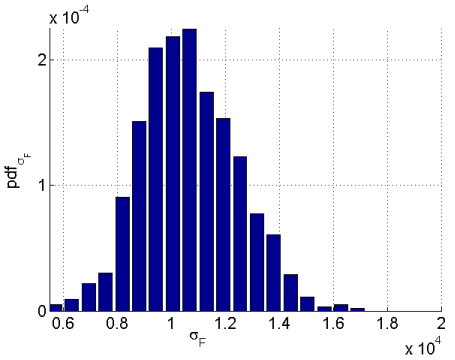

Figure 12: Probability density function for the variance of the frequency (σ_F) for the low Reynolds case

Fig.13 where it can be seen that the computed intermittency agrees well with the experimental data in the first part of the transition region that is between $0 < P < 0.5$. On the other hand, the agreement is not as good in the second half of the transition region. This is due to the noise η which characterizes the experimental data. The error bars represent the uncertainty of the measurements, what we called the noise η, which linearly grows in the transitional zone. In fact, when the noise vanishes the agreement is almost perfect as shown for the forward problem (see Fig. 9). For the current case $n = 5000$ samples are used for the MCMC approach which is enough to guarantee the convergence. For the estimation of the steady state, the *Geweke's* [13] test has been used. This consists in splitting the samples in three parts. The first 20% of them represent the "burn-in" period which groups the number of samples necessary to assess the random walk of the MCMC method towards the exact solution. This first percentage is not considered in the final solution. The reamaining samples correspond to the 60% and the 20% of the total. The *Geweke's* test says that convergence is achieved if the mean of both distributions is approximately the same. In our case, with $n = 5000$ samples the variation on the mean μ_F is 0.1% while the variation on the variance σ_F is 3% between the last two groups of samples.

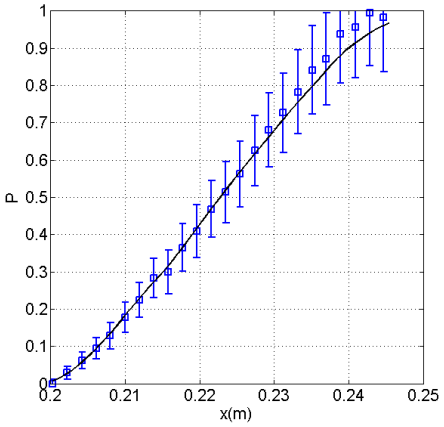

Figure 13: Intermittency as a function of the streamwise location. Comparison of the experimental data with respect to the probability of transition obtained from MCMC.

5. Conclusions

Deterministic tools and a probabilistic approach has been combined to predict laminar to turbulent transition in high speed flows. The method has been applied to experimental data available at the VKI for laminar transition studies on a cone model. Applications have been presented in terms of the *forward problem* and of the *inverse problem*.

In the *forward problem*, we assumed a distribution for the input uncertainties and, using the e^N transition prediction method, we retrieved the probability of transition or intermittency curve γ. The comparison with experimental data at different Reynolds number has demonstrated the validity of the approach for high speed flows. It should therefore be possible to use the intermittency distributions in order to improve existing transitional models. In fact, in the present case, only the Reynolds number was varied between the different cases but other parameters can vary as well, for example the Mach number. A database of intermittency distribution can be built for different conditions

and used to predict transition in numerical simulations. The idea is to use the database validated through comparison with experiments to extrapolate the transition onset in different conditions. In particular, the integration of this approach into existing transitional model for RANS simulations, will be studied in future works.

On the other hand, the *inverse problem* allows to infer disturbance spectra at a location upstream of the transition onset using measured intermittency curves. In the *forward problem*, intermittency curves are computed for a given disturbance spectrum by using LST. The inverse method applies a statistical analysis based on the MCMC method and it has been illustrated using one of the experimentally measured data in the VKI-H3 facility.

For the test case, good agreement was found between the given noisy intermittency curve and the curve resulting from inferred spectra. This suggests that the forward model is able to represent the intermittency curve sufficiently well.

These data will be processed and then used in future works for a better comparison with the results of the inverse analysis. Results could be also improved by using a higher-fidelity forward model since LST lacks in capturing the later stage of the transition process. Moreover, the present method relies on a number of assumptions, including the shape of the pdf for the frequency, as well as the kind and number of parameters that are inferred. The effect of these assumptions should carefully be assessed in future works.

6. Acknowledgement

This research has been financed by the **FRIA-FNRS 2012 fellowship**, annual fellowship of the *Fonds de la Recherche Scientifique* (F.R.S.) for doctoral students.

Results presented in the article has been obtained during the **CTR-Summer Program** 2012 at Stanford University (CA). The author would like to thank Dr. Olaf Marxen, Prof. Gianluca Iaccarino, Dr. Catherine Gorle and Dr. Paul Constantine for their fundamental contribution.

References

[1] Anderson J. D., *Hypersonic and High Temperature Gas Dynamics*, AIAA 1986.

[2] Arnal D., *Laminar Turbulent Transition Problem in Supersonic and Hypersonic Flows*, ONERA.

[3] Arnal D.,*Special Course on Progress in Transition Modeling*, AGARD report 793, 1993.

[4] Beckwith E., Creel T., Chen Fang-Jenq, Kendall J., *Free-Stream Noise and Transition Measurements on a Cone in a Mach 3.5 Pilot Low-Disturbance Tunnel*, NASA Technical Paper 2180, September 1983.

[5] Berlin S., *Oblique Waves in Boundary Layer Transition*, Doctoral Thesis, Stockholm, 1998.

[6] Bertin J., Cummings R. M., *Fifty years of hypersonic:when we've been and we're going*, Departments of Aeronautics, United States Air Force Academy, USAF Academy, CO 80840, USA.

[7] Chang, C.L. & Malik, M. R. *Oblique-mode breakdown and secondary instability in a supersonic boundary layers using nonlinear PSE*, Instability, Transition and Turbulence, Hussaini, M. Y., Kumar, A. & Streett, C. L., editors, pp. 231-241. Springer-Verlag, 1992.

[8] Chang, C.-L. & Malik, M. R. *Oblique-mode breakdown and secondary instability in supersonic boundary layer*, J. Fluid Mech. 273, pp. 323-360, 1994.

[9] Constantine P., *Lectures on Uncertainty Quantification, ME470*, Stanford University, May 2012.

[10] Dilley A.D.,*Evaluation of CFD turbulent heating prediction techniques and comparison wit hypersonic experimental data*, NASA/CR-2001-210837.

[11] Fei Li, Choudhari M., Chang C.L., Kimmel R. and Adamczak D., *Hypersonic Transition Analysis for HIFiRE Experiments*, Hypersonic Laminar-Turbulent Transition Meeting, San Diego, California, April 16-19, 2012.

[12] Ferrier M., *Analyse de la stabilité et prévision de la transition laminaire-turbulent de lécoulement proche paroi sur l'avantcorps d'un véhicule hypersonique*, PhD Thesis in Fluid Mechanics, Université d' Orléans, 2008.

[13] Geweke, J., *Evaluating the Accuracy of Sampling-Based Approaches to the Calculation of Posterior Moments*, Bayesian Statistics 4, Oxford: Oxford University Press, 169-193, 1992

[14] Gorle C., Emory M. and Iaccarino G., *Epistemic uncertainty quantification of RANS modeling for an underexpanded jet in a supersonic cross flow*, Center for Turbulence Research Annual Research Briefs 2011.

[15] W.K. Hastings, *Monte carlo sampling methods using markov chains and their applications*, Biometrika 57, 97109, 1970.

[16] Horvath T.J., Berry S.A., Hollis B.R., Chang C.L. and Singer B.A., *Boundary layer transition on slender cones in conventional and low disturbance Mach 6 wind tunnels*, NASA Langley Research Center, AIAA 2002-2743.

[17] Kendall J.M., *An experimental investigation of leading edge shock wave-boundary layer interaction at hypersonic speeds*, PhD thesis, California Institute of Technology, 1956.

[18] Iaccarino G., Eldred M., Doostan A., Ghattas O., *Introduction to Uncertainty Quantification*,SIAM CSE Conference, Miami, FL, 2009.

[19] Iaccarino G., Pettersson P., Nordstr J. & Witteveen J., *Numerical methods for uncertainty propagation in high speed flows*,V European Conference on Computational Fluid Dynamics, ECCOMAS CFD 2011, Lisbon, Portugal, 14-17 June 2010.

[20] Lees, L., *The Stability of the Laminar Boundary Layer in a Compressible Fluid*, NACA Report No. 876, 1947.

[21] Loeven G.J.A., Witteveen J.A.S. & Bijl H., *Probabilistic Collocation: An Efficient Non-Intrusive Approach For Arbitrarily Distributed Parametric Uncertainties*, AIAA 2007-317, 45th AIAA Aerospace Sciences Meeting and Exhibit, January 2007, Reno, Nevada.

[22] Mack L. M., *Boundary layer stability theory*, 1969, JPL, Report 900-277.

[23] Mack, L. M., *Linear Stability Theory and the Problem of Su-*

personic Boundary-Layer Transition, AIAA Journal., Vol. 13, No.3, pp 278-289, March 1975.

[24] Mack, L. M., *Boundary Layer Linear Stability Theory*, AGARD Report No.70g, June 1984.

[25] Malik M. R., *Instability and transition in supersonic boundary layers*, Energy Sources Technology Conference, New Orleans, LA, February 1984.

[26] Masutti D., *Natural and induced transition on a 7° half-cone at Mach 6*, Proceedings of the 2012 VKI PhD. Symposium, von Karman Institute for Fluid Dynamics, 2012.

[27] Marxen O., Iaccarino G. & Shaqfeh E., *Boundary-layer transition via spatially growing oblique waves*, under consideration for publication in Journal of Fluid Mechanics, 2011.

[28] Mayer C., Von Terzi D. & Fasel H., *Direct numerical simulation of complete transition to turbulence via oblique breakdown at Mach 3*, J. Fluid Mech., 2011.

[29] McDaniel, R.D., Nance, R.P. and Hassan, H.A, (2000), *Transition Onset Prediction for High-Speed Flow* , Journal of Spacecraft and Rockets, Vol. 37, No. 3, May-June, 2000.

[30] Narasimha R.,*On the distribution of intermittency in the transition region of a boundary layer*, Journal of Aeronautical Science, vol. 24, pp. 711-712, 1957.

[31] Pecnik R., Witteveen J. & Iaccarino G., *Uncertainty quantification for laminar-turbulent transition prediction in RANS turbomachinery applications*, 49th AIAA Aerospace Sciences Meeting including the New Horizons Forum and Aerospace Exposition, Orlando, Florida, AIAA 2011-660.

[32] Pinna F., *Numerical study of stability of flows from low to high Mach number*, PhD Thesis, von Karman Institute for Fluid Dynamics and Universitá di Roma 'La Sapienza', 2012.

[33] Reshotko E., *Transition Prediction: Supersonic and Hypersonic Flows*, RTO-EN-AVT-151.

[34] Sankaran S. & Marsden A. L., *A Stochastic Collocation Method for Uncertainty Quantification and Propagation in Cardiovascular Simulations*, Journal of Biomechanical Engineering, March 2011, Vol. 133.

[35] H. Schlichting, *Boundary Layer Theory*, Springer,1955.

[36] Schneider S.P., *Hypersonic Laminar-Turbulent Transition on Circular Cones and Scramjet Forebodies*, Progress in Aerospace Sciences, Vol. 40, pp. 1-50, 2004.

[37] Schneider S.P., *Flight Data for Boundary-Layer Transition at Hypersonic and Supersonic Speeds*, Journal of Spacecraft and Rockets, Vol. 36, No. 1, January-February 1999.

[38] Robarge T.W. and Schneidert S.P., *Laminar Boundary-Layer Instabilities on Hypersonic Cones: Computations for Benchmark Experiments*, AIAA Paper 2005-5024, 35th Fluid Dynamics Conference, Toronto, June 2005.

[39] Serino G., Marxen O., Pinna F., Rambaud P. & Magin T., *Transition prediction for oblique breakdown in supersonic boundary layers with uncertain disturbance spectrum*, AIAA 20122973 pp. 111, 2012.

[40] Stetson K.F., *Hypersonic Boundary layer Transition*, Advances in hypersonic, 1992.

[41] Stetson K.F. and G. H. Rushton, *Shock tunnel investigation of boundary-layer transition at Mach 5.5*, AIAA Journal, May 1967.

[42] Tarantola A., *Inverse problem theory and methods for model parameters estimation*, Siam, 1987.

[43] Tumin A., Wang X. and Zhong X., *Direct numerical simulation and the theory of receptivity in a hypersonic boundary layer*, Physics of fluids, vol. 19, 2007.

[44] van Ingen J.L., *The eN method for transition prediction : Historical review of work at TU Delft*, 38th Fluid Dynamics Conference and Exhibit, 23 - 26 June 2008, Seattle, Washington.